AGU PUBLICATIONS

Geophysical Research Letters

RESEARCH LETTER
10.1002/2017GL073535

Key Points:
- Simultaneous simulation of the GrIS and AIS over the warm Pliocene
- Pliocene time slice MIS KM5c displays limited ice volume fluctuations
- Asynchronous response in ice volume to orbital forcing during MIS K1

Supporting Information:
- Supporting Information S1
- Movie S1
- Movie S2

Correspondence to:
B. de Boer,
b.deboer@uu.nl

Citation:
de Boer, B., Haywood, A. M., Dolan, A. M., Hunter, S. J., & Prescott, C. L. (2017). The transient response of ice volume to orbital forcing during the warm late Pliocene. *Geophysical Research Letters*, *44*, 10,486–10,494. https://doi.org/10.1002/2017GL073535

Received 21 MAR 2017
Accepted 7 OCT 2017
Accepted article online 16 OCT 2017
Published online 30 OCT 2017

The Transient Response of Ice Volume to Orbital Forcing During the Warm Late Pliocene

Bas de Boer[1,2], Alan M. Haywood[2], Aisling M. Dolan[2], Stephen J. Hunter[2], and Caroline L. Prescott[2]

[1]Institute for Marine and Atmospheric research Utrecht, Utrecht University, Utrecht, Netherlands, [2]School of Earth and Environment, University of Leeds, Leeds, UK

Abstract Examining the nature of ice sheet and sea level response to past episodes of enhanced greenhouse gas forcing may help constrain future sea level change. Here, for the first time, we present the transient nature of ice sheets and sea level during the late Pliocene. The transient ice sheet predictions are forced by multiple climate snapshots derived from a climate model set up with late Pliocene boundary conditions, forced with different orbital forcing scenarios appropriate to two Marine Isotope Stages (MISs), MIS KM5c, and K1. Our results indicate that during MIS KM5c both the Antarctic and Greenland ice sheets contributed to sea level rise relative to present and were relatively stable. Insolation forcing between the hemispheres was out of phase during MIS K1 and led to an asynchronous response of ice volume globally. Therefore, when variations of precession were high, inferring the behavior of ice sheets from benthic isotope or sea level records is complex.

1. Introduction

A rise in global mean sea level due to the melting of ice sheets on Antarctica and Greenland is related to a warming climate (Masson-Delmotte et al., 2013). However, the magnitude and rates of change of the Antarctic and Greenland ice sheets (AIS and GrIS) in response to warming remain only partially constrained. A better understanding of the response of the ice sheets to increasing temperature is needed to make more rigorous projections of how much sea level change could be expected in the future (e.g., Kennicutt et al., 2014). A warm interval within the late Pliocene (3.264 to 3.025 million years before present) can be used to gain a better understanding of the response of the ice sheets to a warming climate with concentrations of atmospheric CO_2 close to or higher than present (Haywood, Dowsett, & Dolan, 2016; Martinez-Boti et al., 2015). During this interval, atmospheric CO_2 varied significantly (between 300 and 450 ppmv) and to a certain degree coincident with orbital parameters and thus insolation. Proxy data from deep-ocean sediments suggest a warming and/or reduction of ice volume relative to the present during discrete stages within the interval (Figure S1 in the supporting information), giving way to a rise in global mean sea level (Miller et al., 2012).

For this interval, the largest increase in global mean sea level relative to the present could reflect a minimum in ice volume on both Antarctica and Greenland. Alternatively, an analysis of insolation variability (Dolan et al., 2011; Raymo et al., 2006) indicates that an asynchronous response of ice sheets in the Northern Hemisphere (NH) and Southern Hemisphere (SH) might be expected, where variations of the orbital parameters yield globally nonuniform changes in solar radiative forcing at the top of the atmosphere (Dolan et al., 2011).

Previous simulations of sea level change for the Pliocene have largely focused on the equilibrium response of ice sheets to snapshot simulations of general circulation models (GCMs) using fixed boundary conditions (e.g., orbit, CO_2) (e.g., De Boer et al., 2015; Dolan et al., 2011; Hill et al., 2010; Koenig et al., 2015). Although these studies provide an initial estimate of the response of the AIS and GrIS to a particular climate generated by a GCM, they lack the transient behavior that inherently contributes to past climate variability (e.g., Smith & Gregory, 2012). A number of transient simulations with three-dimensional (3-D) ice sheet models do capture the transient nature of Antarctic (Pollard & DeConto, 2009, 2012) and global ice volume (De Boer et al., 2014). However, computational costs of an interactively coupled ice sheet model—GCM transient simulations are too great for such long (10^5–10^6 years) experiments. Therefore, climate variability in these studies is highly parameterized.

Table 1
Setup of the Transient Experiment

Phase	Time (Ma)	Forcing	Initial ice	Ice sheets
1. Spin-up	3.500–3.226	LR04 + PI HadCM3	present day	AIS, GrIS, NaIS, EuIS
2. MIS KM5c	3.226–3.184	HadCM3	last time step phase 1	AIS, GrIS
3. Transition	3.184–3.082	LR04 + PI HadCM3	last time step phase 2	AIS, GrIS, NaIS, EuIS
4. MIS K1	3.082–3.038	HadCM3	last time step phase 3	AIS, GrIS
c. Control	*0.410–0.0*	*LR04 + PI HadCM3*	*present day*	*AIS, GrIS, NaIS, EuIS*

Note. LR04 is the Lisiecki and Raymo (2005) benthic δ^{18}O record, from which a uniform temperature anomaly is derived and applied to the preindustrial (PI) HadCM3 climatology (see text). The last entry in Table 1 is the control experiment. This is given in italic emphasis to show that it is not part of the four-step experiment for the Pliocene but is a separate experiment.

We present a first step toward a fully coupled system of ice volume and climate variability across the late Pliocene. We use a 3-D ice sheet model to simulate ice volume over Greenland and Antarctica, forced with multiple snapshot experiments of an Atmosphere-Ocean GCM (Prescott et al., 2014). The ice sheet model simulations are driven by 21 snapshot GCM experiments across Marine Isotope Stage (MIS) KM5c, from 3.226 to 3.184 million years ago (Ma), and 11 snapshot experiments across MIS K1, from 3.082 to 3.038 Ma. The interglacial events targeted in Prescott et al. (2014) were chosen specifically because KM5c represents a period of relatively stable orbit with similar to modern insolation forcing (see also Haywood, Dolan, et al., 2013) and K1 is a warm interglacial event which has been also targeted by the PLIOMAX sea level project (Raymo et al., 2009). For each interval of 40,000 year (40 kyr) the snapshot GCM simulations are forced with the same boundary conditions for CO_2 and ice sheet topography but use different orbital parameters associated with the specific time point within the 40 kyr intervals (Prescott et al., 2014).

A large difference in orbital forcing can be seen when comparing MIS KM5c and K1 (Figure S1 in the supporting information). As demonstrated in Prescott et al. (2014), the different orbital forcing across MIS KM5c and K1 leads to a significant difference in changes in predicted surface-air temperatures (Figures S2–S11 in the supporting information). The model simulations presented here attempt to capture the transient response of climate and ice volume to orbital variations, whereas the responses and feedbacks associated with changes in atmospheric CO_2, vegetation, and ice sheet topography are not included in these experiments.

2. Methods

2.1. Experimental Design

The transient experiments we conducted specifically focus on the late Pliocene, starting at 3.5 Ma and ending just after MIS K1 at 3.038 Ma. The simulations are set up in four phases but run continuously in time (Table 1). For the *spin-up phase* from 3.5 to 3.226 Ma and the *transition phase* from 3.184 to 3.082 Ma, we employ an inverse method as used previously in De Boer et al. (2013, 2014) to derive a temperature anomaly to calculate ice volume over four ice sheet regions: Antarctica, Greenland, North America, and Eurasia. As in De Boer et al. (2014) we include all four ice sheet regions to capture the full scale of sea level variations during these periods. The inverse method uses the benthic δ^{18}O LR04 stack (Lisiecki & Raymo, 2005) to force the *spin-up* and *transition* phases only, from which we derive a surface-air temperature anomaly from the difference between modeled and observed benthic δ^{18}O (Text S1 in the supporting information). At 3.5 Ma, the ice sheets are initialized from their present-day conditions, with the initial AIS adopted from Bedmap2 (Fretwell et al., 2013) and initial GrIS adopted from Bamber et al. (2001) (Figure S12 in the supporting information). The temperature anomaly derived from the change in benthic δ^{18}O LR04 data is added to the preindustrial monthly temperature climatology of HadCM3 (as used in De Boer et al., 2015) for the *spin-up* and *transition phases* only, assuming a spatially and seasonally uniform temperature change. We also conducted a control experiment over four glacial cycles running from 410 kyr ago to the present to demonstrate the efficacy of the modeling framework (Table 1).

For both MIS KM5c (from 3.226 to 3.184 Ma) and MIS K1 (from 3.082 to 3.038 Ma), we only use output from the Atmosphere-Ocean GCM HadCM3 (Prescott et al., 2014) to provide climate forcing for the ice sheet models, and not make use of the LR04 benthic stack. Here we specifically focus on the AIS and GrIS (Table 1) as simulations have shown that little to no ice will grow over Eurasia and North America using the specific HadCM3

climate forcing employed here. The HadCM3 simulations used fixed Pliocene boundary conditions based on the Pliocene Model Intercomparison Project (PlioMIP) as described in Haywood et al. (2011), for which atmospheric trace gases were set to preindustrial levels, except the CO_2 concentration was set to 405 ppmv and orbital parameters were varied accordingly. The simulations as presented in Prescott et al. (2014) were carried out 20 kyr on either side of MIS KM5c and K1, separated by 2 and 4 kyr, respectively. In total, the 21 runs for KM5c and 11 runs for K1 differ only in the orbital parameters tied to the specific time point (see Tables S1 and S2 in the supporting information).

The ice sheet model simulations for Greenland and Antarctica for MIS KM5c and K1 were carried out continuously, restarting from the final time step of the *spin-up* and *transition phase* and changing the climate model forcing every 2 and 4 kyr, respectively, not using the LR04 benthic stack (Table 1). For all simulations we use the climatological averages derived from the final 100 years of each HadCM3 experiment, which are then kept fixed for each 2 and 4 kyr time period forcing the ice sheet models, centered around the time point shown in Tables S1 and S2 in the supporting information. We use monthly mean surface-air temperature and precipitation from HadCM3 only to drive the surface mass balance, and for the AIS we also use depth-dependent ocean temperatures for calculating oceanic refreezing/melt at the bottom of the ice shelves (Figures S2–S11 in the supporting information). In contrast to the *spin-up* and *transition phase*, which are forced by both the preindustrial climate of HadCM3 changed with a temperature anomaly derived from the benthic δ^{18}O LR04 stack, the experimental simulations across KM5c and K1 are forced by HadCM3 alone and are therefore independent of the benthic stack.

2.2. The Ice Sheet Model

For the ice sheet simulation we use the 3-D thermomechanical ice sheet model ANICE, part of the IMAU-ICE package (De Boer et al., 2013, 2014). The model employs a combination of the shallow ice and shallow shelf approximations (SIA and SSA, respectively) to simulate ice flow over land and floating ice. Basal stresses are included in the SSA in order to simulate the basal sliding velocities (De Boer et al., 2013; Martin et al., 2011). The model horizontal resolution is 20 km for the GrIS and 40 km for the AIS, the North American Ice Sheet (NaIS), and Eurasian Ice Sheet (EuIS). Ice sheet grids are defined as in De Boer et al. (2013) using an oblique stereographic projection. Spatial interpolation of topography and climate fields is achieved using OBLIMAP v2.0 (Reerink et al., 2016).

We use a bedrock model that incorporates the bedrock deformation due to changes in ice loading with a function consisting of a generalized term for the shape of the deformation and a time response term (De Boer et al., 2013). We do not include ice shelves for the GrIS, but basal velocities are calculated using the SSA. For all regions we employ the same surface mass balance scheme, basing surface snow melting on monthly insolation and temperature variations (Text S2.1 in the supporting information). Precipitation changes within the ice sheet model are calculated as a function of the change in temperature, which in turn is corrected for variability in surface elevation following a constant lapse rate of 8 K km^{-1}. Next, accumulation of snow is obtained as a temperature-dependent fraction of the total precipitation. We base melting or refreezing of ocean water underneath the ice shelves of the AIS on a heat transfer equation (Text S2.2 in the supporting information), for which we use the 3-D annual mean ocean temperatures of the climate model (De Boer et al., 2013, 2015).

2.3. Sensitivity Tests

For both the full transient Pliocene experiment and the control experiment over the past four glacial cycles (Table 1), we have conducted 32 different sensitivity experiments, varying five parameters in the ice sheet model with each having two different values (Table S4 in the supporting information). We have selected this particular set of variables based on previous experiments with Antarctica (Maris et al., 2014), previous transient simulations (De Boer et al., 2014) and tuning with the specific preindustrial climate of HadCM3 for the last four glacial cycles (Figure S13 in the supporting information). The five parameters that are varied are (i) the surface ablation constant controlling the amount of surface melt (Text S2.1 in the supporting information); (ii) the sub–ice shelf melt parameter controlling the melt/refreezing underneath the floating ice shelves (Text S2.2 in the supporting information); (iii) the enhancement factor for SIA flow controlling the ice flow on land (Text S2.3 in the supporting information, following Ma et al. (2010)); (iv) the enhancement factor for SSA flow controlling ice flow for ice streams and shelves (Text S2.3 in the supporting information, following Ma et al. (2010)); and (v) the minimum till friction angle controlling the amount of basal friction at the base of the ice sheets (Text S2.4 in the supporting information).

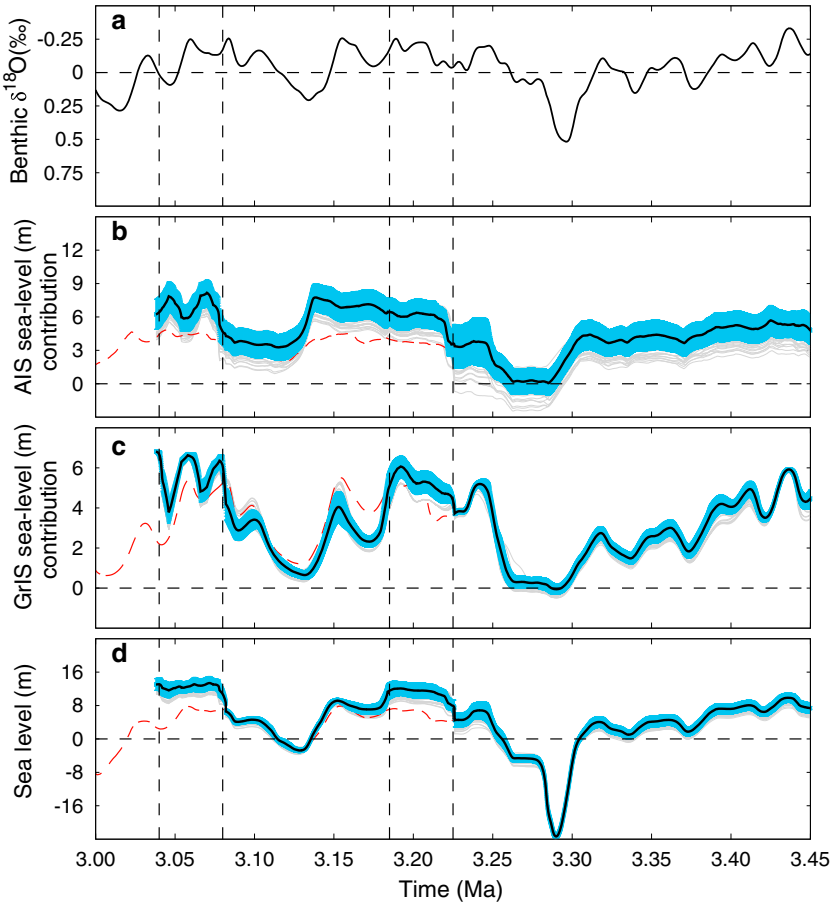

Figure 1. All transient simulations for the Pliocene. (a) Benthic δ^{18}O stacked record (Lisiecki & Raymo, 2005) relative to present. Contributions to global mean sea level from (b) the AIS and (c) the GrIS. (d) Total change in global mean sea level relative to present day. In all panels the 32 sensitivity simulations are shown in gray; the thick black line represents the reference simulation and blue shading the standard deviation based on the ensemble. The vertical dashed lines denote MIS KM5c from 3.224 to 3.126 Ma and MIS K1 from 3.082 to 3.038 Ma. The dashed red line represents a continuous simulation just using LR04 as forcing with the reference settings.

3. Transient Simulations and Sensitivity Experiments

From the results of the control simulation over the past four glacial cycles (Figure S13 in the supporting information), we have selected one reference experiment from the set of 32 experiments with the specific parameter settings given in bold in Table S4 in the supporting information. The reference simulation is selected based on three criteria calculating specific ice sheet variables at the last time step, $t = 0$ kyr, relative to the present-day observed ice sheets (Figure S12 in the supporting information). The difference in (i) ice area of the ice shelves of the AIS, (ii) land-based ice of the AIS and GrIS, and (iii) sea level contribution of both the final ice sheets is smallest at $t = 0$ kyr in the control simulation. In terms of contribution to global mean sea level, the differences for the AIS (−0.30 m sea level equivalent (s.l.e.)) and the GrIS (+0.02 m s.l.e.) are relatively small. The *spin-up* and *transition phase* of the transient simulations for the Pliocene include all four ice sheets and hence simulate the total change in global mean sea level. These simulations are driven by changes in benthic δ^{18}O, which is largely reflected in the simulated global mean sea level (Figures 1a and 1d) that is calculated from the change in ice volume of all four ice sheets, relative to the present.

The variability within the ensemble is demonstrated by the standard deviation that is calculated relative to the reference simulation (blue shading in Figure 1). The standard deviation is on average relatively small over the full simulation (1.14 m for the total change in global mean sea level). During MIS KM5c and K1, which are forced by HadCM3 only,, the differences within the ensemble are slightly larger with a standard deviation of 1.65 and 1.51 m for total global mean sea level, respectively. The spread between model simulations is largely due to differences between simulated ice volume of the AIS, whereas the variance for the GrIS is considerably smaller

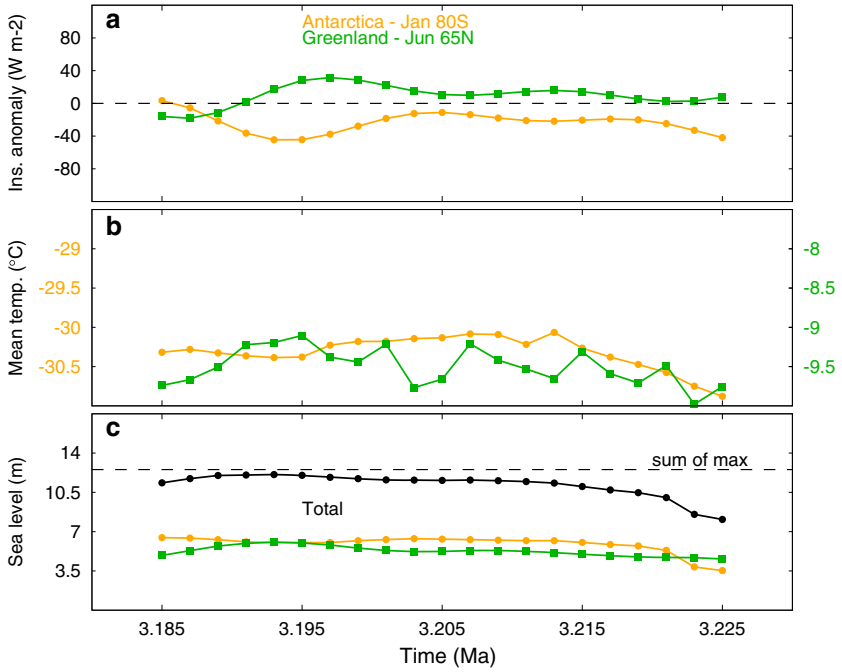

Figure 2. Forcing and model response for MIS KM5c, from 3.225 to 3.185 Ma. (a) Insolation anomaly relative to present over Antarctica, January 80°S in orange with dots and over Greenland, June 65°N in green with squares (Laskar et al., 2004). (b) Mean annual temperature over Antarctica in orange with dots (using the left *y* axis) and Greenland in green with squares (using the right *y* axis), averages for all land points in HadCM3. (c) Simulated global mean sea level change every 2 kyr from the AIS in orange with dots, GrIS in green with squares and total in black. Sea level changes are the final values after each 2 kyr interval of a constant HadCM3 forcing and shown here on the central time point of the HadCM3 simulations (see Table S1 in the supporting information). In Figure 2c the horizontal dashed line indicates the sum of the maximum contributions of the AIS (at 3.185 Ma) and GrIS (at 3.193 Ma) within the time frame.

(Figures 1b and 1c). During MIS KM5c and K1 the standard deviations for the AIS and the GrIS contributions to global mean sea level are 1.22–1.25 m and 0.52–0.37 m, respectively. Although the difference between the simulated GrIS contribution to sea level across the multiple simulations is small, the size of the ice sheet varies considerably during the late Pliocene, ranging from near present-day ice extent at 3.3 Ma to almost no ice at the end of MIS KM5c (3.184 Ma) and during MIS K1 (from 3.082 to 3.038 Ma). As we simulate here, the contribution to sea level change is the same order of magnitude for both the GrIS and AIS.

The difference in standard deviation between the four phases of the transient simulation can be ascribed to the different methodologies applied. During the *spin-up* and *transition phase*, we calculate one single temperature anomaly derived from the benthic LR04 stack, which is applied as a spatially uniform temperature change everywhere on the preindustrial climatology of HadCM3. Also, the parameter values are not changed for the EuIS and NaIS which hence dampens the variability within the ensemble and explains the lower standard deviation outside the MIS KM5c and K1 intervals. To emphasize the added value of using HadCM3 climate forcing during MIS KM5c and K1 only, illustrated with the vertical dashed lines, a continuous simulation using the spatially uniform temperature anomaly derived from LR04 is shown in red (Figure 1). The changes within both 40 kyr intervals are solely driven by the HadCM3 changes, independent of the benthic LR04 stack, and hence do resemble more realistic global nonuniform changes in temperature and ice volume. For both MIS KM5c and K1 using the HadCM3 Pliocene forcing provides a more direct response to the orbital variations and yields higher simulated global mean sea level contributions. Specifically for MIS K1, the final global mean sea level contributions are largely underestimated when not using the HadCM3 forcing (3.038 Ma in red in Figures 1b–1d).

4. The Ice Volume Response During Pliocene Interglacials

4.1. Ice Volume During MIS KM5c

MIS KM5c has been identified as an important time slice for simulating Pliocene climate because the orbital forcing was largely similar to present day (Haywood, Dolan, et al., 2013). As we show here, insolation does not

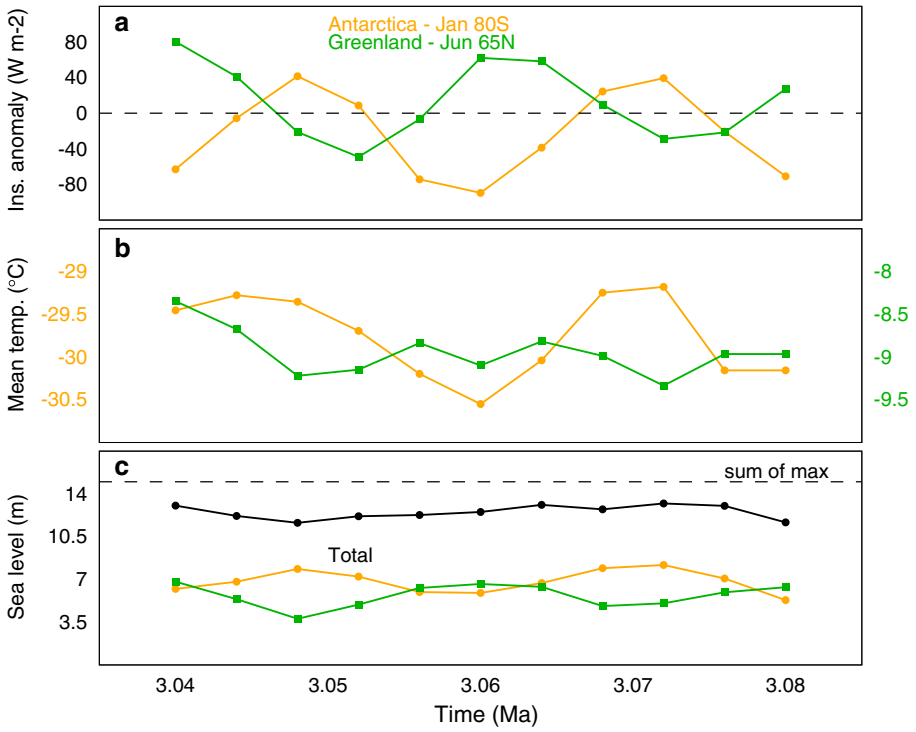

Figure 3. Forcing and model response for MIS K1, from 3.080 to 3.040 Ma. (a) Insolation anomaly over Antarctica, January 80°S in orange with dots and over Greenland, June 65°N in green with squares (Laskar et al., 2004). (b) Mean annual temperature over Antarctica in orange with dots (left *y* axis) and Greenland in green with squares (right *y* axis), averages for all land points in HadCM3. (c) Simulated global mean sea level change every 4 kyr from the AIS in orange with dots, GrIS in green with squares, and total in black. Sea level changes are the final values after each 4 kyr interval of a constant HadCM3 forcing and shown here on the central time point of the HadCM3 simulations (see Table S2 in the supporting information). In Figure 3c the horizontal dashed line indicates the sum of the maximum contributions of the AIS (at 3.072 Ma) and GrIS (at 3.040 Ma) within the time frame.

vary greatly over the course of the 40 kyr time slice, between −45 and +3 W m^{-2} over Antarctica and −18 and +32 W m^{-2} over Greenland (Figure 2a). Similarly, the response in both annual mean temperatures over Antarctica and Greenland (Figures S2 and S5 in the supporting information) and the changes in ice volume can be considered stable, especially from 3.213 to 3.193 Ma (Figures 2b and 2c).

In light of our presented results, it is encouraging for data-model comparison, and the forthcoming second phase of PlioMIP (Haywood, Dowsett, Dolan, et al., 2016), to know that within the time slice of KM5c the variability of ice volume can be considered small. As a possible large contribution to polar amplification and long-term climate sensitivity (Haywood, Hill, et al., 2013; Köhler et al., 2015), the variability of ice sheets and hence sea level during this time is modest. Moreover, CO_2 is kept fixed in the HadCM3 snapshot simulations, and the variance of atmospheric CO_2 proxy estimates during mid-MIS KM5c likewise appears to be small, although data coverage in CO_2 reconstructions remains sparse (Badger et al., 2013; Martinez-Boti et al., 2015). This low variability is supported by other reconstructions and simulations of atmospheric CO_2 (Stap et al., 2016; Van de Wal et al., 2011) (Figure S1d in the supporting information).

4.2. Ice Volume During MIS K1

In contrast to MIS KM5c, the variability in orbital forcing during K1 is much more pronounced due to a higher value of eccentricity; that is, a more elliptical orbit around the Sun leads to a higher amplitude of precession. Hence, insolation (here shown as anomalies relative to present) varies between −90 and +42 W m^{-2} over Antarctica and −50 and +80 W m^{-2} over Greenland (Figure 3a), a range almost twice as large as during MIS KM5c. Consequently, changes in surface-air temperature both across Antarctica and Greenland are large and closely reflect the variability seen in insolation at the top of the atmosphere (Figures 3b and S7 and S10 in the supporting information).

Variations of annual mean temperatures averaged over all land are 3 times larger during MIS K1 relative to MIS KM5c. Importantly, the large variability seen during MIS K1 leads to an asynchronous response in predicted ice volume in our simulations (Figure 3c). The changes as simulated here in surface-air temperature and ice volume during MIS K1 can be largely linked to changes in precession (modulated by eccentricity), which is out of phase between hemispheres, with two distinct maxima in precession within the 40 kyr interval at 3.05 and 3.072 Ma (Figure S1b in the supporting information). A precession maximum corresponds to the longest day during SH summer being at perihelion, the point closest to the Sun on the ellipse. Hence, SH summer receives more solar insolation (Figure S1 in the supporting information).

5. Discussion and Conclusions

Here we have focused on two interglacial intervals during the late Pliocene, MIS KM5c and K1. Whereas MIS KM5c is characterized by limited ice volume and global mean sea level fluctuations, during MIS K1 the AIS and GrIS vary out of phase, with maxima and minima of the AIS and GrIS not occurring at the same time. For MIS KM5c, the maximum sea level contributions of the AIS (at 3.185 Ma) and the GrIS (at 3.193 Ma) are 8 kyr apart but both at the end of the MIS KM5c interval. Previous simulations have largely focused on the equilibrium response of both the GrIS and AIS to a particular climatology. However, as we show here, the sum of the largest contribution to global mean sea level (dashed line in Figure 2c) is always larger during MIS KM5c than the actual total simulated change in global mean sea level. Although insolation variations are of opposite signal, variability in ice volume during the MIS KM5c interval is low and does not change significantly after the initial response to the imposed HadCM3 climate forcing at the start of the interval.

As proposed by Dolan et al. (2011), which focused on the equilibrium response of ice volume, the maximum global mean sea level high stand may not occur at a maximum in insolation in either hemisphere. Our results from MIS K1 support this supposition, where the sum of the largest contributions to sea level change (dashed line in Figure 3c) is much larger than the actual total change in global mean sea level. Most notably, the maximum contribution of the AIS (at 3.072 Ma) is 32 kyr earlier than that of the GrIS (3.040 Ma). The maximum total change in global mean sea level during MIS K1 in the reference experiment is 13.39 m at 3.072 Ma.

Antarctic ice volume variability shown during MIS K1 is also reflected in the ice discharge simulated by the ice sheet model, which follows the advance and retreat of the AIS (Figures S14b and S14c in the supporting information). Observed iceberg-rafted debris (IBRD) from site U1361 offshore of the Wilkes Land margin (Patterson et al., 2014) shows a double peak during MIS K1 (Figure S14d in the supporting information). Although the peaks in IBRD could be visually correlated with maxima in summer insolation (see Figure 2 in Patterson et al. (2014)), we here observe that simulated ice discharge increases when the AIS is advancing, actually corresponding to a lowering of summer insolation (Figure S14a in the supporting information). However, several processes that are involved such as precise drifting of icebergs following ocean circulation, a more sophisticated calving law, feedback of ice topography on the climate, or variations in atmospheric CO_2 are missing in the current analysis. Both IBRD from site U1361 and our simulated ice discharge do depict a strong variability during MIS K1. As opposed to MIS KM5c and K1 using HadCM3 climate forcing only, during the *spin-up* and *transient phase* the response to orbital forcing is not included in our simulations. This can be largely ascribed to our methodology applied, using a single spatially uniform temperature anomaly, which misses the influence of insolation variations on temperature when using GCM simulations.

We use the suite of 32 simulations to more closely examine the variability within the ensemble, representing the uncertainty in parameterizations. The minimum change in global mean sea level during MIS K1 occurs at the beginning of the interval at 3.082 Ma for all 32 simulations. On the other hand, the maximum change in global mean sea level occurs at two distinct time periods: either around 3.072 Ma, coinciding with a peak in precession and the smallest AIS, or around 3.040 Ma, which coincides with peak warming over Greenland and the smallest GrIS. Looking at the sea level extremes within the ensemble, the highest and lowest maximum sea levels are 14.21 and 10.67 m, respectively (Figure S15 and Table S5 in the supporting information). Sea level change relative to present is predominantly caused by a retreated West AIS (WAIS) and a generally lower East AIS (EAIS). The GrIS has retreated almost entirely, with only several scattered ice caps remaining on the eastern side of the island. The difference between minima in simulated sea level during MIS K1 is less for which the highest and lowest minimum sea levels during MIS K1 are 9.47 and 7.14 m, respectively (Figure S16 and Table S5 in the supporting information). During minima in sea level, the WAIS is retreated slightly, with a partially intact Filchner-Ronne ice shelf. The GrIS still contributes significantly but consists of a single ice sheet

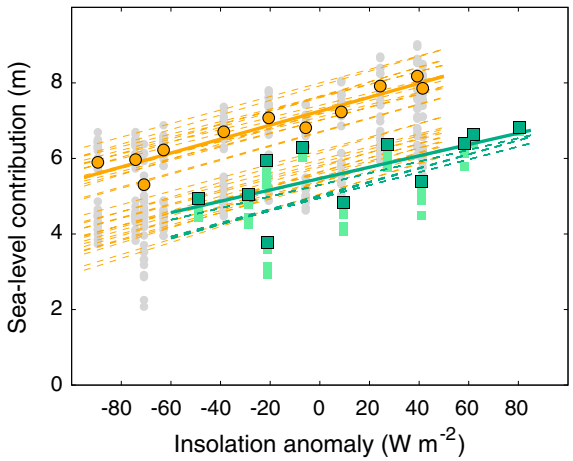

Figure 4. Cross plot of sea level contributions of the AIS and GrIS relative to the insolation used in the HadCM3 simulations for MIS K1 (Figures 3a and 3c). Simulated ice volume for the AIS (GrIS) and corresponding insolation anomaly relative to present of January 80°S (June 65°N) are shown in orange dots (green squares). Bold symbols are the reference simulation; all other 31 simulations are given in gray (AIS) and light green (GrIS). Linear fit lines for the reference experiments are shown by the thick lines (R^2 for the AIS is 0.90 and for the GrIS is 0.46); dashed lines are the fitted lines for the sensitivity experiments.

on the southeastern side of the island. The estimated total change in global mean sea level from our reference experiment, with standard deviation, is 13.39 ± 1.58 m at 3.072 Ma during MIS K1. This falls within the range estimated from Miller et al. (2012) at approximately the same time, 20.65 ± 8.6 m (1 standard deviation).

The model realization which simulated the highest sea level rise, relative to the reference experiment, used (i) a higher value of the enhancement factor for shelf flow and (ii) a lower value of the friction angle for basal till, that is, making the base more slippery (Table S5 in the supporting information). These two parameters generate a higher outflow of ice across the grounding line, thus leading to more ice loss particularly on Antarctica. The simulation with lower sea level rise occurs using (i) a lower value of the surface ablation constant, (ii) a lower value of the sub ice-shelf melt factor, and (iii) a lower value of the enhancement factor for SIA ice flow (Table S5 in the supporting information). These model settings lead to less melt and a more stagnant ice sheet, with a lower outflow across the grounding line.

The response of ice volume to the early summer insolation anomaly during MIS K1 shows a strong linear fit for the AIS with a R^2 value of 0.90 and a fair fit for the GrIS with a R^2 value of 0.46 (Figure 4). For all ensemble members, a similar fit is realized, ranging between 0.62 and 0.92 for the AIS and between 0.38 and 0.49 for the GrIS. Generally speaking, higher (lower) than present insolation over either Antarctic or Greenland results in an increase (decrease) in the contribution to global mean sea level as we have simulated here. This is independent of the physical parameterizations used in the model, for which all 32 ensemble runs show a similar behavior of ice sheet response. The precise contributions do depend on transient effects embedded in the continuous simulations. Moreover, the level of atmospheric CO_2 used in the HadCM3 simulations of 405 ppmv leads to an increase in ice loss as seen for MIS KM5c (Figure 2), for which additional variability is added when changes in insolation relative to the present are higher such as during MIS K1 (Figure 3).

Prescott et al. (2014) showed that the multiple snapshot HadCM3 simulations do not predict globally synchronous temperatures during the MIS KM5c and K1 intervals. Our simulations indicate that the hypothesis put forward by Raymo et al. (2006) of an asynchronous response of ice sheets combined with our transient modeling is indeed a key factor in predicting orbital timescale sea level for warmer than present climate, in particular, the warm Pliocene. This is predominantly the case for time periods with a higher value of eccentricity, that is, a more elliptical orbit, giving way to large variability in precession, which is out of phase between hemispheres, hence leading to an antiphase response between the NH and SH. As proposed by Raymo et al. (2006) this leads to a weak precessional signal in observed benthic $\delta^{18}O$ records. Therefore, when precession variability is large, caution is advised when directly inferring the behavior of ice sheets from oxygen isotope records in the Pliocene. Moreover, simply summing the maximum individual contribution of the Greenland and Antarctic ice sheets to global mean sea level rise during the MIS K1 interval is shown to be larger than the actual total global mean sea level rise. The out of phase behavior of precession thus leads to an asynchronous response of the AIS and GrIS during the late Pliocene that could counteract their contributions to global mean sea level change.

Acknowledgments
This project has received funding from the European Union's Horizon 2020 research and innovation program under the Marie Sklodowska-Curie grant agreement 660814. B. de Boer is currently funded by NWO Earth and Life Sciences (ALW), project 863.15.019. A. M. Haywood, A.M. Dolan, S. J. Hunter, and C. L. Prescott acknowledge funding from the European Research Council under the European Union's Seventh Framework Programme (FP7/2007-2013)/ERC grant agreement 278636, as well as the EPSRC-supported Past Earth Network. All ice sheet model simulations were undertaken on ARC2, part of the High Performance Computing facilities at the University of Leeds, UK. Model data are available upon request. Ice sheet model output is available on the author's website and on the data repository Pangaea.

References

Badger, M. P. S., Schmidt, D. N., Mackensen, A., & Pancost, R. D. (2013). High-resolution alkenone palaeobarometry indicates relatively stable pCO_2 during the Pliocene (3.3–2.8 Ma). *Philosophical Transactions of the Royal Society A: Mathematical, Physical and Engineering Sciences*, *371*(2001), 20130094.

Bamber, J. L., Layberry, R. L., & Gogineni, S. P. (2001). A new ice thickness and bed data set for the Greenland ice sheet 1. Measurements, data reduction, and errors. *Journal of Geophysical Research*, *106*, 33,773–33,780.

De Boer, B., Dolan, A. M., Bernales, J., Gasson, E., Goelzer, H., Golledge, N. R., … van de Wal, R. S. W. (2015). Simulating the Antarctic ice sheet in the late-Pliocene warm period: PLISMIP-ANT, an ice-sheet model intercomparison project. *The Cryosphere*, *9*(3), 881–903. https://doi.org/10.5194/tc-9-881-2015

De Boer, B., Lourens, L. J., & van de Wal, R. S. W. (2014). Persistent 400,000-year variability of Antarctic ice volume and the carbon-cycle is revealed throughout the Plio-Pleistocene. *Nature Communications*, *5*, 2999. https://doi.org/10.1038/ncomms3999

De Boer, B., van de Wal, R. S. W., Lourens, L. J., Bintanja, R., & Reerink, T. J. (2013). A continuous simulation of global ice volume over the past 1 million years with 3-D ice-sheet models. *Climate Dynamics*, *41*(5–6), 1365–1384.

Dolan, A. M., Haywood, A. M., Hill, D. J., Dowsett, H. J., Hunter, S. J., Lunt, D. J., & Pickering, S. J. (2011). Sensitivity of Pliocene ice sheets to orbital forcing. *Palaeogeography, Palaeoclimatology, Palaeoecology*, *309*, 98–110. https://doi.org/10.1016/j.palaeo.2011.03.030

Fretwell, P., Pritchard, H. D., Vaughan, D. G., Bamber, J. L., Barrand, N. E., Bell, R., … Zirizzotti, A. (2013). Bedmap2: Improved ice bed, surface and thickness datasets for Antarctica. *The Cryosphere*, *7*(1), 375–393.

Haywood, A. M., Dolan, A. M., Pickering, S. J., Dowsett, H. J., McClymont, E. L., Prescott, C. L., … Valdes, P. J. (2013). On the identification of a Pliocene time slice for data–model comparison. *Philosophical Transactions of the Royal Society A: Mathematical, Physical and Engineering Sciences*, *371*, 2001.

Haywood, A. M., Dowsett, H. J., & Dolan, A. M. (2016). Integrating geological archives and climate models for the mid-Pliocene warm period. *Nature Communications*, *7*, 10646. https://doi.org/10.1038/ncomms10646

Haywood, A. M., Dowsett, H. J., Dolan, A. M., Rowley, D., Abe-Ouchi, A., Otto-Bliesner, B., … Salzmann, U. (2016). The Pliocene Model Intercomparison Project (PlioMIP) phase 2: Scientific objectives and experimental design. *Climate of the Past*, *12*(3), 663–675.

Haywood, A. M., Dowsett, H. J., Robinson, M. M., Stoll, D. K., Dolan, A. M., Lunt, D. J., … Chandler, M. A. (2011). Pliocene Model Intercomparison Project (PlioMIP): Experimental design and boundary conditions (Experiment 2). *Geoscientific Model Development*, *4*(3), 571–577.

Haywood, A. M., Hill, D. J., Dolan, A. M., Otto-Bliesner, B. L., Bragg, F., Chan, W. L., … Zhang, Z. (2013). Large-scale features of Pliocene climate: Results from the Pliocene Model Intercomparison Project. *Climate of the Past*, *9*(1), 191–209.

Hill, D. J., Dolan, A. M., Haywood, A. M., Hunter, S. J., & Stoll, D. K. (2010). Sensitivity of the Greenland Ice Sheet to Pliocene sea surface temperatures. *Stratigraphy*, *7*(2-3), 111–122.

Kennicutt, M. C. I., Chown, S. L., Cassano, J. J., Liggett, D., Peck, L. S., Massom, R., … Sutherland, W. J. (2014). A roadmap for Antarctic and Southern Ocean science for the next two decades and beyond. *Antarctic Science*, *27*, 1–16. https://doi.org/10.1017/S0954102014000674

Koenig, S. J., Dolan, A. M., de Boer, B., Stone, E. J., Hill, D. J., DeConto, R. M., … van de Wal, R. (2015). Ice sheet model dependency of the simulated Greenland ice sheet in the mid-Pliocene. *Climate of the Past*, *11*(3), 369–381.

Köhler, P., de Boer, B., von der Heydt, A. S., Stap, L. B., & van de Wal, R. S. W. (2015). On the state dependency of the equilibrium climate sensitivity during the last 5 million years. *Climate of the Past*, *11*(12), 1801–1823.

Laskar, J., Robutel, P., Joutel, F., Gastineau, M., Correia, A., & Levrard, B. (2004). A long-term numerical solution for the insolation quantities of the Earth. *Astronomy & Astrophysics*, *428*, 261–285.

Lisiecki, L., & Raymo, M. (2005). A Pliocene-Pleistocene stack of 57 globally distributed benthic δ^{18}O records. *Paleoceanography*, *20*, PA1003. https://doi.org/10.1029/2004PA001071

Ma, Y., Gagliardini, O., Ritz, C., Gillet-Chaulet, F., Durand, G., & Montagnat, M. (2010). Enhancement factors for grounded ice and ice shelves inferred from an anisotropic ice-flow model. *Journal of Glaciology*, *56*, 805–812.

Maris, M. N. A., de Boer, B., Ligtenberg, S. R. M., Crucifix, M., van de Berg, W. J., & Oerlemans, J. (2014). Modelling the evolution of the Antarctic ice sheet since the last interglacial. *The Cryosphere*, *8*(4), 1347–1360.

Martin, M. A., Winkelmann, R., Haseloff, M., Albrecht, T., Bueler, E., Khroulev, C., & Levermann, A. (2011). The Potsdam Parallel Ice Sheet Model (PISM-PIK)—Part 2: Dynamic equilibrium simulation of the Antarctic ice sheet. *The Cryosphere*, *5*(3), 727–740.

Martinez-Boti, M. A., Foster, G. L., Chalk, T. B., Rohling, E. J., Sexton, P. F., Lunt, D. J., … Schmidt, D. N. (2015). Plio-Pleistocene climate sensitivity evaluated using high-resolution CO_2 records. *Nature*, *518*(7537), 49–54.

Masson-Delmotte, V., Schulz, M., Abe-Ouchi, A., Beer, J., Ganopolski, A., Rouco, J. G., … Timmermann, A. (2013). Information from paleoclimate archives. In Stocker, T., Qin, D., Plattner, G.-K., Tignor, M., Allen, S., Boschung, J., ..., & Midgle, P. (Eds.), *Climate change 2013: The physical science basis. Contribution of working group I to the fifth assessment report of the Intergovernmental Panel on Climate Change* (pp. 383–464). Cambridge, UK: Cambridge University Press.

Miller, K. G., Wright, J. D., Browning, J. V., Kulpecz, A., Kominz, M., Naish, T. R., … Sosdian, S. (2012). High tide of the warm Pliocene: Implications of global sea level for Antarctic deglaciation. *Geology*, *40*(5), 407–410.

Patterson, M. O., McKay, R., Naish, T., Escutia, C., Jimenez-Espejo, F. J., Raymo, M. E., … IODP Expedition 318 Scientists (2014). Orbital forcing of the East Antarctic ice sheet during the Pliocene and Early Pleistocene. *Nature Geoscience*, *7*(11), 841–847.

Pollard, D., & DeConto, R. M. (2009). Modelling West Antarctic ice sheet growth and collapse through the past five million years. *Nature*, *458*, 329–332. https://doi.org/10.1038/nature07809

Pollard, D., & DeConto, R. M. (2012). Description of a hybrid ice sheet-shelf model, and application to Antarctica. *Geoscientific Model Development*, *5*, 1273–1295. https://doi.org/10.5194/gmd-5-1273-2012

Prescott, C. L., Haywood, A. M., Dolan, A. M., Hunter, S. J., Pope, J. O., & Pickering, S. J. (2014). Assessing orbitally-forced interglacial climate variability during the mid-Pliocene Warm Period. *Earth and Planetary Science Letters*, *400*, 261–271. https://doi.org/10.1016/j.epsl.2014.05.030

Raymo, M. E., Hearty, P., Conto, R. D., O'Leary, M., Dowsett, H., Robinson, M., & Mitrovica, J. (2009). PLIOMAX: Pliocene maximum sea level project. *PAGES News*, *17*(2), 58–59.

Raymo, M., Lisiecki, L., & Nisancioglu, K. (2006). Plio-Pleistocene ice volume, Antarctic climate, and the global δ^{18}O record. *Science*, *313*, 492–495.

Reerink, T. J., van de Berg, W. J., & van de Wal, R. S. W. (2016). OBLIMAP 2.0: A fast climate model–ice sheet model coupler including online embeddable mapping routines. *Geoscientific Model Development*, *9*(11), 4111–4132.

Smith, R. S., & Gregory, J. (2012). The last glacial cycle: transient simulations with an AOGCM. *Climate Dynamics*, *38*, 1545–1559.

Stap, L. B., de Boer, B., Ziegler, M., Bintanja, R., Lourens, L. J., & van de Wal, R. S. W. (2016). CO_2 over the past 5 million years: Continuous simulation and new δ^{18}B-based proxy data. *Earth and Planetary Science Letters*, *439*, 1–10.

Van de Wal, R. S. W., de Boer, B., Lourens, L. J., Köhler, P., & Bintanja, R. (2011). Reconstruction of a continuous high-resolution CO_2 record over the past 20 million years. *Climate of the Past*, *7*(4), 1459–1469.